Progress In Electromagnetics Research C, Vol. 137, 199–209, 2023

Compact Wideband Four Elements MIMO Antenna for 5G Applications

Shubhangi M. Verulkar, Alka Khade, Mahadu Trimukhe, and Rajiv K. Gupta*

Abstract—A compact four-element multiple-input multiple-output (MIMO) antenna is proposed for 5G applications. The offset fed antenna structure is designed from a rectangular and semicircular monopole antenna. In this novel MIMO structure, the surface current and near fields of left element are mainly concentrated toward left and that of right element towards right, and thus high isolation is achieved between left and right elements even without using any isolation technique, whereas the little surface current at the nearby edges of top and bottom elements helps in achieving high isolation. The fabricated prototype has board dimensions of $0.374\lambda_0 \times 0.275\lambda_0$, where λ_0 is the free-space wavelength at 3.3 GHz. The structure offers isolation > 20 dB between the elements over 3.3–6.3 GHz. The envelope correlation coefficient (ECC), diversity gain (DG), and mean effective gain (MEG) conform to MIMO antenna specifications. The antenna offers stable nearly omnidirectional radiation patterns.

1. INTRODUCTION

Multiple-input multiple-output (MIMO) technology plays a crucial role in wireless communication systems as it enhances the performance of the system by offering high data rate, high throughput, and large channel capacity. MIMO technology involves multiple antennas at both transmitter and receiver ends. As a result, it not only offers high data rate but also mitigates fading effect. MIMO technology is extensively employed in 4G and 5G applications.

5G technology, unlike its previous generations, provides connectivity to everyone at any place at any time. It offers high data rate with low latency and reliable access for seamless connectivity required for video streaming and similar applications. These features are extremely important for virtual reality, augmented reality, and virtual business. 5G technology is going to impact the economy of a country and the world as a whole.

Antennas are vital and thus designed to provide better performance, and enhanced functionality of the systems. To reduce the size of portable devices, small size antennas are desired. Compact dual band antenna using slot and split ring resonators (SRRs) and ultra-wide band (UWB) antenna with band notch characteristics are designed for multiband applications [1–3]. A dual band antenna with metamaterial cell is designed, and reconfigurable UWB characteristics are obtained using PIN diodes [4]. However, MIMO antenna system requires multiple antennas, and these multiple antennas, when being positioned in a size-constraint system, significantly degrade its performance due to mutual coupling. Therefore, the researchers are forced to design small size MIMO antennas with high isolation.

Sub-6 GHz 2-element MIMO antenna systems have been reported [5–8]. A T-shaped corrugated strip is placed between semi-circular radiators in [5], whereas a T-shaped junction and two rectangular and annular ring slots at the center of the partial ground [6] are used to achieve high isolation. Wide band coplanar waveguide (CPW)-fed ship-shaped 2-element MIMO antenna on isolated ground [7] and

Received 15 May 2023, Accepted 25 August 2023, Scheduled 13 September 2023

* Corresponding author: Rajiv Kumar Gupta (rajivgupta@ternaengg.ac.in).
The authors are with the Department of Electronics and Telecommunication, Terna Engineering College, Navi-Mumbai, India.

a tri-band 2-element MIMO antenna using a stub in ground plane and feed line [8] are designed to offer high isolation.

Four elements MIMO antennas have been proposed for wireless applications and 5G technology [9–16]. A square-shaped four elements MIMO antenna with offset feedline and defected ground structure (DGS) is designed [9]. A quad port orthogonal elliptical tree shape MIMO antenna operates over 4.2–13.2 GHz [10]. The antenna has large dimensions but offers isolation > 25 dB. A MIMO antenna consisting of fractal circular ring radiators on trapezoid-shaped partial ground plane with a notch is reported. The elements are configured in plus shape on isolated ground to obtain isolation > 20 dB [11]. A P-shaped antenna with partial ground for 5G applications offers isolation > 28 dB [12]. Octagon-shaped [13] and CPW feed [14] UWB MIMO antennas have been reported; however, these structures have large size. Elements of a UWB MIMO antenna are designed on top and bottom layers using a decoupling structure [15]. Elements of a UWB MIMO antenna are placed orthogonally, and metal vias are used. T and rectangular slits and a triangular chamfer in ground are etched to improve bandwidth and isolation [16]. The antenna has small dimensions; however, it is difficult to fabricate and suffers from design complexity. 8-elements MIMO antenna systems for sub-6 GHz bands with different isolation and impedance matching techniques have been reported in [17–20]. MIMO antennas operating over 5G millimeter waves frequency bands are designed in [21–23].

In this article, a compact four elements MIMO antenna is proposed for 5G sub-6 GHz applications. The novel structure employs neither any isolation techniques nor any meta-material or split ring resonator (SRR) yet offers high isolation. It is simple to design and have smaller dimensions than the reported structures [9–23]. The offset fed antenna structure is designed from a rectangular and semicircular monopole antenna. In this novel MIMO structure, the surface current and near fields of left element are mainly concentrated toward left and that of right element towards right, and thus high isolation is achieved between left and right elements even without using any isolation technique, whereas the little surface current at the nearby edges of top and bottom elements helps in achieving high isolation. The designed structure operates over 3.3 to 6.3 GHz and has FR4 board dimensions of $0.374\lambda_0 \times 0.275\lambda_0$. It offers nearly omnidirectional radiation characteristics.

The rest of the paper is organized as follows. Section 2 of the paper deals with antenna geometry, evolution steps, two elements and four elements MIMO antennas. MIMO system performance parameters are discussed in Section 3. Section 4 deals with measurement results. The proposed antenna is compared with the antennas reported in the literature in Section 5. The conclusion is provided in Section 6.

2. ANTENNA DESIGN

2.1. Single Element Wideband Antenna

Figure 1 depicts the geometry of the wideband antenna, and Table 1 lists its detailed dimensions. The evolution stages of this antenna are shown in Fig. 2. An offset fed miniaturized wideband antenna is evolved from a rectangular monopole antenna (RMPA) to operate over 3.3–6.4 GHz for 5G sub-6 GHz applications. An RMPA is designed to operate over 5.2–8.0 GHz. The operating frequency band is decreased to 3.3–6.4 GHz by step by step designing process. To decrease the resonant frequency, the ground plane width is decreased, and the gap between the ground plane and radiating patch is increased (Antenna 2). An off-set feed is employed to improve impedance matching. Then a semicircular patch is placed at the top of RMPA to further decrease the lower operating frequency (Antenna 3). A circular slot is etched at the center with little effect on impedance bandwidth (Antenna 4). To enhance the

Table 1. Optimized dimensions of parameters of wideband antenna (in mm).

Wide band Antenna															
W_s	L_s	L_g	W_g	L_{f1}	L_{f2}	W_p	L_p	W_{f1}	W_{f2}	R_1	R_2	S_2	W_1	L_1	S_1
15	10	10	4	3	1	4	8	1	5	4	3.3	1.6	0.5	7.2	1.5

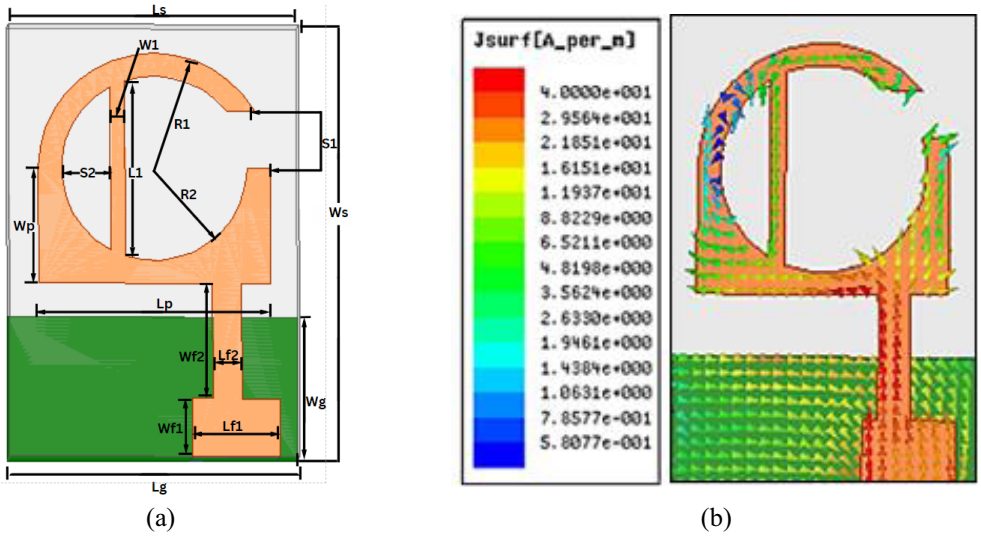

Figure 1. (a) Geometry, (b) surface current distribution of wideband antenna.

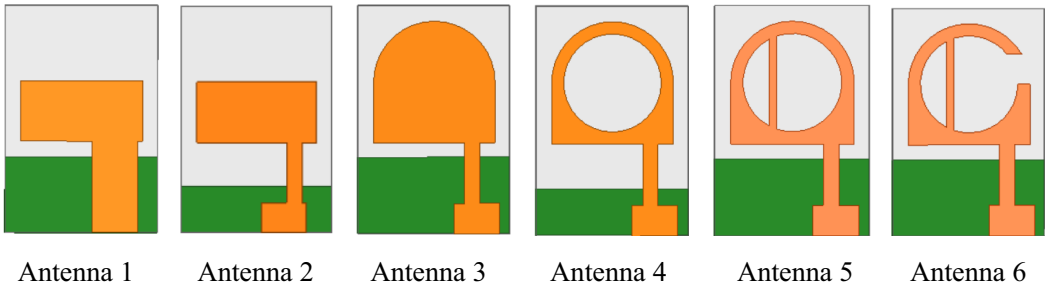

Figure 2. Evolution stages of wideband antenna.

impedance bandwidth, a vertical strip is added at the center (Antenna 5). Finally, a slot is etched in right ring to improve impedance matching (Antenna 6).

Initially, 'Antenna 1' a $4 \times 8\,\text{mm}^2$ rectangular monopole is designed on a $15 \times 10\,\text{mm}^2$ FR4 substrate (1.6 mm thickness, $\varepsilon_r = 4.4$, and $\tan\delta = 0.02$) and simulated using HFSS. The lowest frequency (f_L) at $S_{11} = -9.5\,\text{dB}$ of a printed rectangular monopole antenna (PMRA) is given by [24]

$$f_L = 72/((W + L/2\pi + g) \cdot k)) \text{ when } W > L \tag{1}$$

where the length 'L', width 'W', and the gap 'g' between the ground plane edge and radiating patch are in mm, while f_L is in GHz. $k = 1.15$ for the FR4 substrate [24, 25]. In 'Antenna 1', the simulated and calculated f_L are 5.2 GHz and 5.38 GHz, respectively ($L = 4\,\text{mm}$, $W = 8\,\text{mm}$ and $g = 3\,\text{mm}$). It resonates at 6.55 GHz and $S_{11} \leq -10\,\text{dB}$ over 5.2–8.0 GHz.

To improve impedance matching, an off-set feed with a step is employed in Antenna 2. The off-set feed is employed to ensure that the surface current and near fields are concentrated towards the left which in turn helps in reducing mutual coupling between elements when an element is placed to its right. It resonates at 4.5 GHz and $S_{11} \leq -10\,\text{dB}$ over 3.85–5.4 GHz. In Antenna 3, a semicircular patch of radius 4 mm is placed at the top of Antenna 2. It increases the current path length and inductance of antenna and therefore, results in decrease in resonant frequency. Antenna 3 resonates at 4.1 GHz and $S_{11} \leq -10\,\text{dB}$ over 3.4–5.0 GHz. Return losses S_{11} of these antennas are shown in Fig. 3(a).

Since most of the surface current is concentrated at the periphery, and there is little current at the center of the antenna, a circular slot of radius 3 mm is etched in Antenna 3 to form Antenna 4. There is little effect on the resonant frequency and impedance bandwidth. Antenna 4 resonates at 4.2 GHz, and

$S_{11} \leq -10$ dB over 3.5–5.2 GHz is obtained. In 'Antenna 5', a vertical strip is added in the center of 'Antenna 4'. The resultant two rings resonate at nearby frequencies and couple electromagnetically to provide wide impedance bandwidth [24]. These two rings couple electromagnetically and increase the bandwidth of antenna. Therefore, bandwidth depends on the dimensions and position of vertical strip. Antenna 5 resonates at 3.8 GHz, and $S_{11} \leq -10$dB over 3.15–6.0 GHz is obtained.

In Antenna 6, a slot is etched in the right ring. The slot is equivalent to a capacitor, while the left conducting ring, equivalent to an inductance, loads the right ring, and therefore, this slot improves S_{11} or return loss of the structure [26]. The dimension and position of the slot also affect the electromagnetic coupling between two rings and therefore, the resonant frequency and bandwidth of the antenna. S_{11} plot shown in Fig. 3(b) indicates two resonant frequencies. The surface current density, shown in Fig. 1(b), reveals the two distinct surface current path length and the electromagnetic coupling between the two rings. The parameters of Antenna 6 are optimized to operate over the 5G sub-6 GHz band. Antenna 6 resonates at 4.0 GHz and 5.0 GHz, and $S_{11} \leq -10$ dB over 3.3–6.4 GHz is obtained.

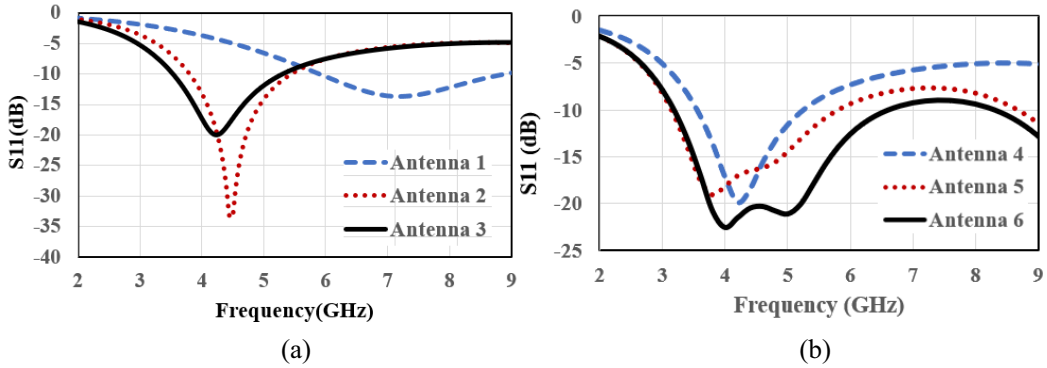

Figure 3. Return Loss S_{11}, (a) Antenna 1, 2, 3 and (b) Antenna 4, 5, 6.

2.2. Two Elements MIMO Antenna

A two-element MIMO antenna is designed using above wideband antenna. The two elements are the mirror image of each other and placed at edge-to-edge distance 'd' as shown in Fig. 4(a). Since the surface current and near field of left antenna is mainly concentrated towards left, and that of right element is towards right, two elements are placed close to each other. The isolation between the two elements is expected to be high even without employing any isolation technique. The effect of edge-to-edge distance 'd' between the two elements is analyzed. The isolation of 20 dB is achieved at $d = 5$ mm which is $0.055\lambda_0$. The antenna operates over 3.3–6.5 GHz. S-parameters for different 'd' are shown in Fig. 4(b). The board dimensions of this 2-element compact MIMO antenna are 15×25 mm^3 or

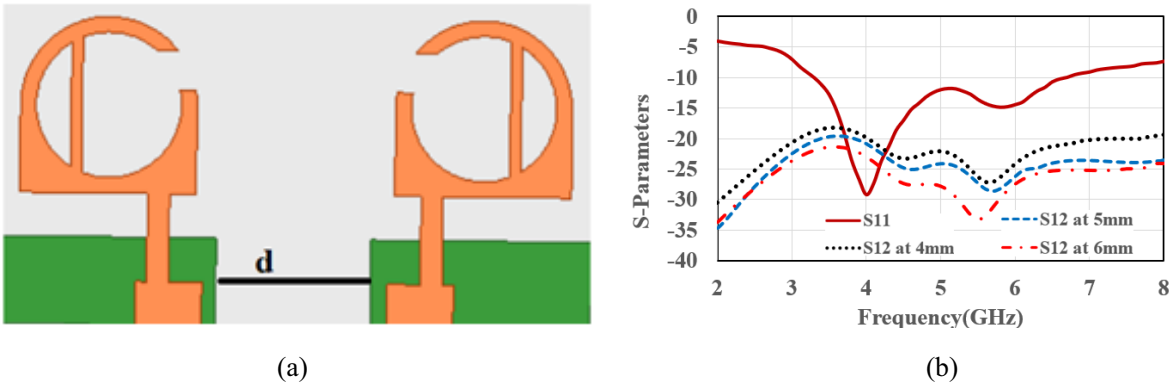

Figure 4. (a) Geometry (b) S_{11} and S_{12} at different d of two element MIMO antenna.

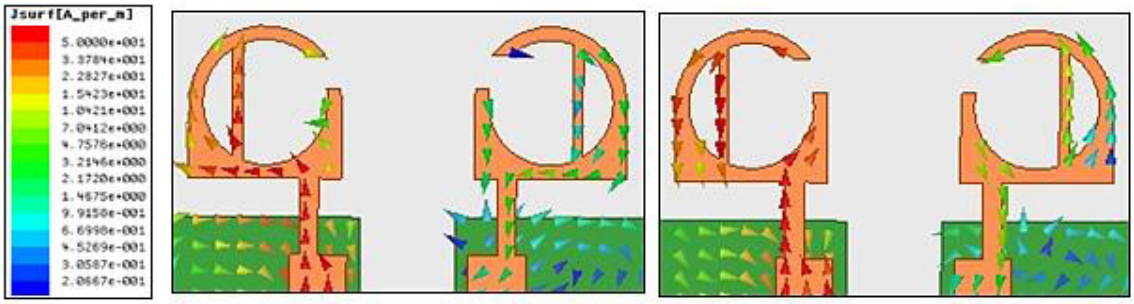

(a) 3.8 GHz (b) 5.8 GHz

Figure 5. Surface current distribution.

$0.165\lambda_0 \times 0.275\lambda_0$.

Mutual coupling can also be analyzed using the surface current distribution. The surface current distributions at 3.8 GHz and 5.8 GHz are shown in Fig. 5. The surface current density on element 2 is more at 3.8 GHz, and it is significantly less at 5.8 GHz. As a result, $S_{12} \leq -20$ dB is obtained at 3.8 GHz, and it improves to -27 dB at 5.8 GHz. As the electrical distance between the two elements increases with frequency, S_{12} decreases with increase in frequency.

The radiation patterns of antenna with port-1 excited and port-2 match-terminated at 3.45 GHz, 5.25 GHz and 5.8 GHz are shown in Fig. 6. Stable and nearly omnidirectional patterns are obtained;

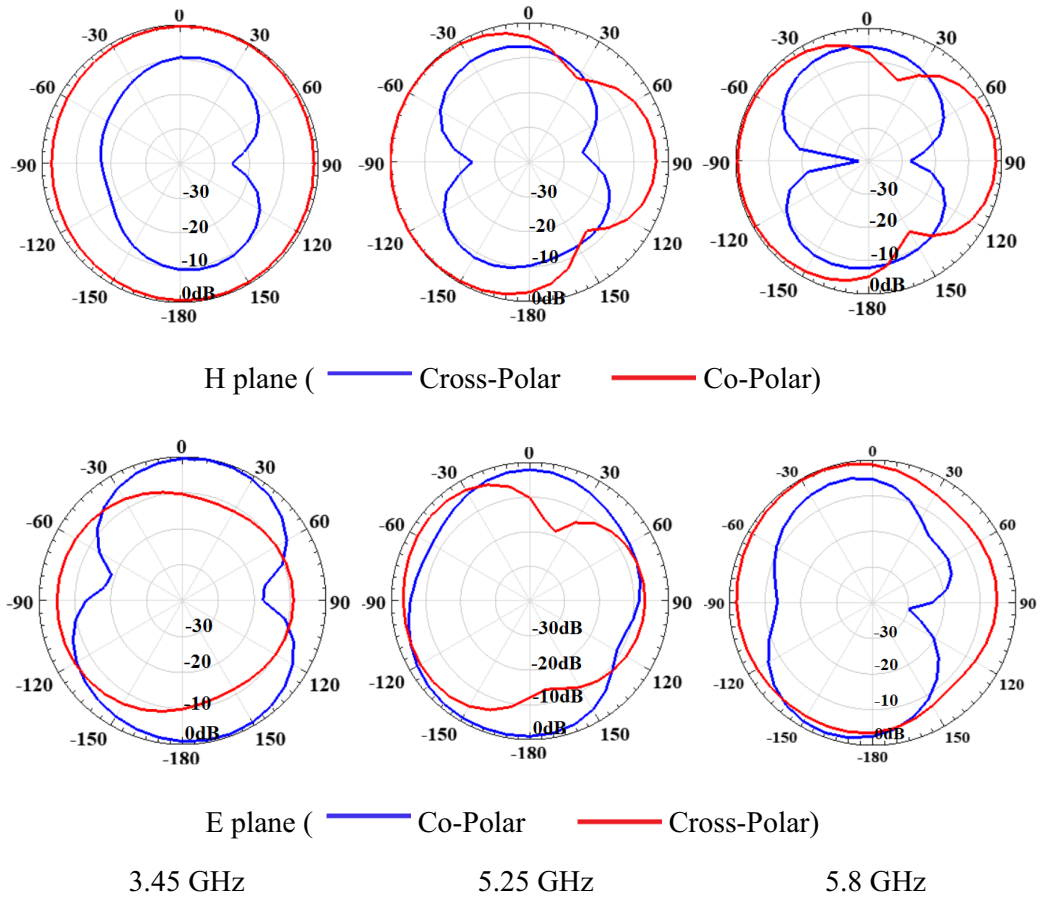

Figure 6. Radiation patterns of 2-elements MIMO antenna.

however, the cross polarization is high, and it increases as the frequency increases due to appreciable surface current in both orthogonal directions. The radiation patterns with port-2 excited and port-1 match-terminated are the mirror image of radiation pattern shown in Fig. 6.

2.3. Four Elements MIMO Antenna Design

Four elements MIMO antenna is designed using a two elements MIMO antenna. The other 2 elements are placed at the top of the previous 2 elements at edge-to-edge distance 'D' as shown in Fig. 7(a). These two elements are the mirror image of the previous two elements. Since the surface current in an element is maximum at the bottom near the feed, and it decreases as one moves away from the feed towards the top, the elements, which are mirror image of each other, are placed with their top portion facing close to each other. The isolation is expected to be high even without employing any isolation technique. The effect of edge-to-edge distance 'D' between the two elements is analyzed. Isolation $>$ 20 dB is achieved at $D = 6$ mm which is $0.066\lambda_0$. The antenna operates over 3.3–6.5 GHz. S-parameters for different 'D' are shown in Fig. 7(b). The board dimensions of this 4-element compact MIMO antenna are $34 \times 25\,\text{mm}^2$ or $0.374\lambda_0 \times 0.275\lambda_0$. The S-parameters of 4-element MIMO antenna structure are shown in Fig. 7(c).

As the four elements are identical and symmetrically placed, there is little variation in return loss at different ports. The proposed MIMO antenna operates ($S_{11}/S_{22}/S_{33}/S_{44}$ <= -10 dB) over 3.3–6.3 GHz and offers isolation $>$ 20 dB as depicted in Fig. 7(c). There is little variation in the return loss at different ports, and therefore only S_{11} and S_{22} are depicted. Similarly, S_{12}, S_{13}, and S_{14} are shown

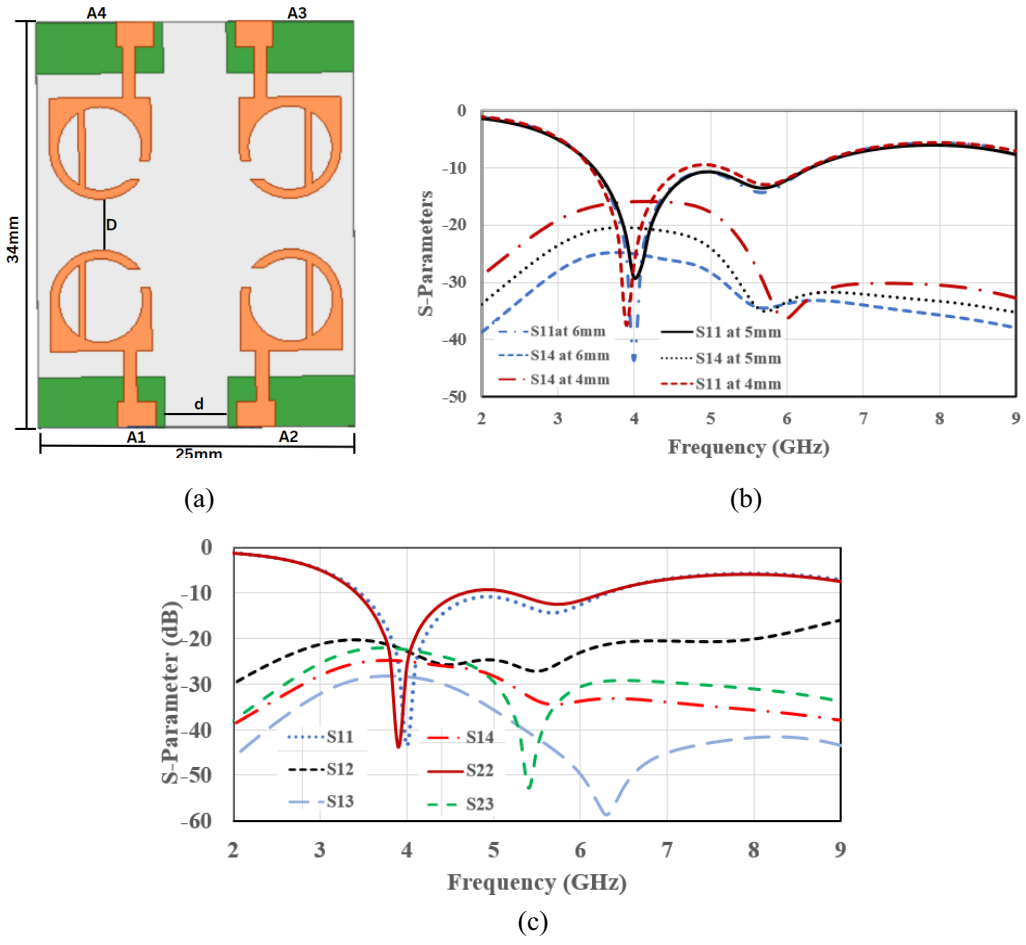

Figure 7. (a) Geometry, (b) S parameters for different D and (c) S-parameters of 4 elements MIMO antenna ($d = 5$ mm, $D = 6$ mm).

in Fig. 7(c). The novelty of the structure lies in the design of a single element which is used to form the MIMO antenna structure. The isolation is > 20 dB over the operating 3.3–6.3 GHz wide band, as the surface current and near fields are mainly concentrated on the left side for the left side elements and on right side for the right-side elements. The elements at the bottom and top have high isolation as the surface current is bound to decrease in each element as one moves away from the feed.

Low mutual coupling in MIMO antenna can be explained by using surface current distribution. The surface current densities at 3.8 GHz and 5.8 GHz are shown in Fig. 8. The antenna element A1 is excited while all other antenna elements are match terminated. At 3.8 GHz, the surface current density induced in element A2 is more than element A4, and it is least in element A3. This is evident from

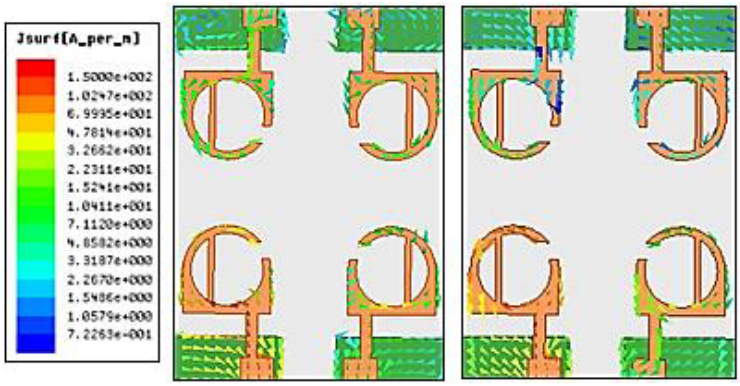

(a) 3.8 GHz (b) 5.8 GHz

Figure 8. Surface current distribution of four elements MIMO antenna.

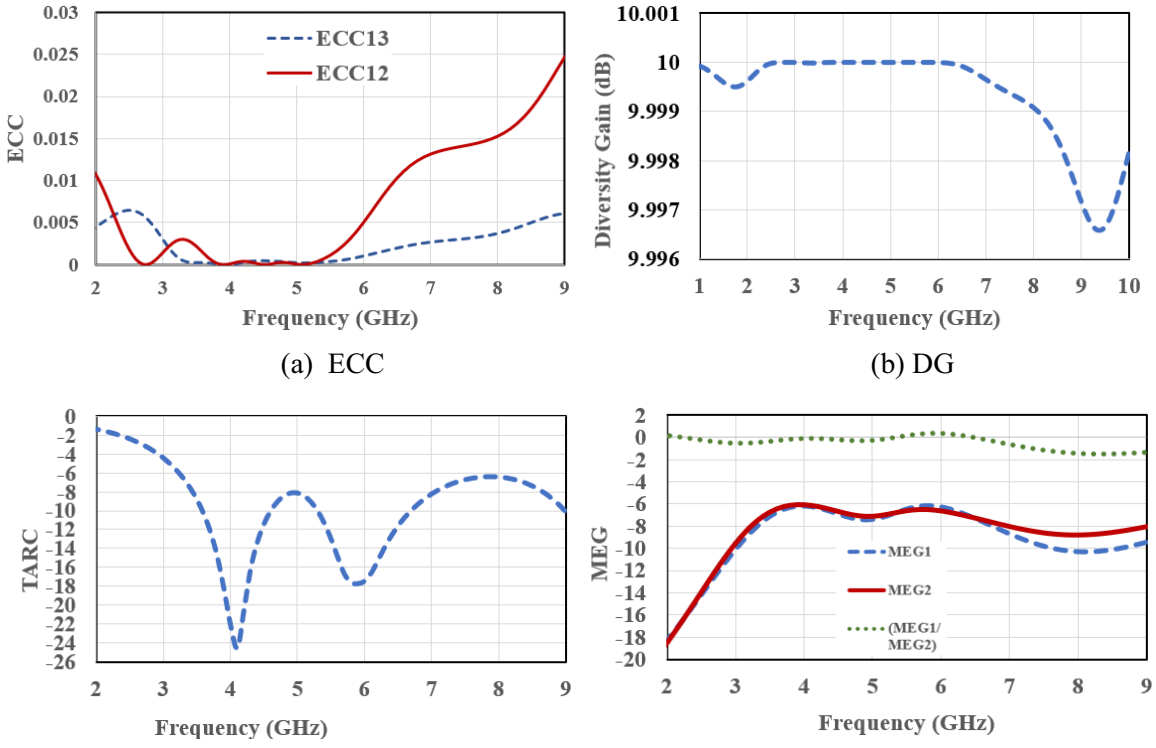

(a) ECC (b) DG

(c) TARC (d) MEG

Figure 9. MIMO parameters of four elements MIMO antenna.

the S parameters as $S_{12} > S_{14} > S_{13}$. At 5.8 GHz, the surface current density in all the elements is comparatively less than the surface current density at 3.8 GHz. As frequency increases, the electric distance between the elements increases. As a result, the mutual coupling at 5.8 GHz is less than the mutual coupling at 3.8 GHz.

3. MIMO SYSTEM PERFORMANCE PARAMETERS

A MIMO antenna structure must adhere to the specifications of key performance parameters such as ECC, total active reflection coefficient (TARC), DG, and MEG to ensure the performance of multichannel system [27]. These parameters are analysed for four element antenna system.

The ECC of proposed structure is < 0.015 over 3–7 GHz which is less than the desired ECC value of 0.5. The calculated diversity gain is approximately 10 dB over 3.3 GHz to 6.3 GHz frequency band indicating good diversity performance of MIMO antenna. MEGs of adjacent elements are approximately equal, and their ratio is close to 0 dB as per the specification of MIMO structure. TARC also satisfies the desired specification. These parameters are shown in Fig. 9.

4. FABRICATION AND MEASURED RESULTS

Figure 10 depicts the fabricated antenna. Agilent 9916A network analyzer is used to measure S-parameters while standard wideband horn antenna is used to measure radiation patterns in an anechoic chamber. Measured and simulated S parameters are in close agreement as shown in Fig. 11. Fig. 12 shows the radiation patterns in X-Z plane (phi = 0°) and Y-Z plane (phi = 90°) at 3.45 GHz, 5.25 GHz,

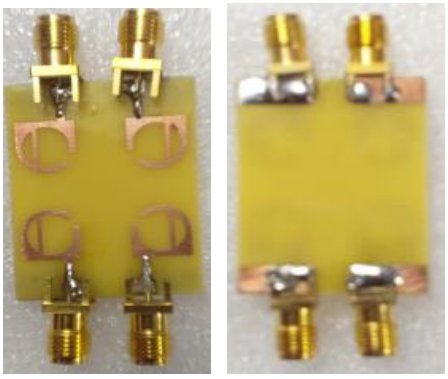

(a) Top-view (b) Bottom-view

Figure 10. Fabricated prototype.

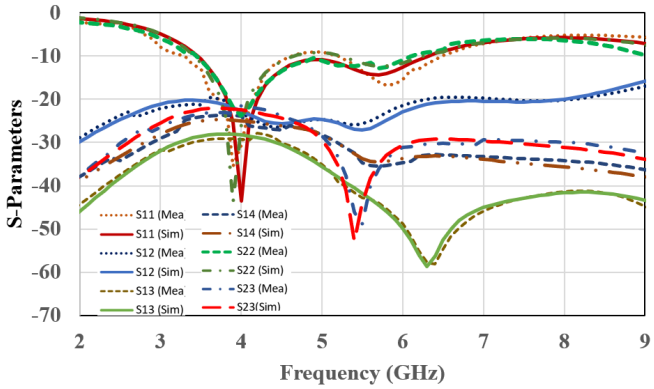

Figure 11. S-parameters of four elements MIMO antenna.

and 5.8 GHz. The radiation patterns are measured with port-1 excited and the other ports matched-terminated. The radiation patterns are stable and omnidirectional.

5. COMPARISON WITH STATE OF ART ANTENNAS

The proposed antenna is compared with reported state of art four and eight elements MIMO antennas with respect to size, frequency band, ECC, and directive gain in Table 2. The proposed antenna is compact and smaller than all other antennas, except [16]. The antenna in [16] has smaller dimensions but difficult to fabricate and suffers from design complexity. The proposed antenna is wideband while that in [16] is ultra-wideband. The proposed structure employs neither any isolation techniques nor any meta-material or SRR and thus, simple to design.

Table 2. Comparison with reported four elements MIMO antennas.

Ref.	Antenna Size (mm × mm)	Bandwidth in GHz	No. of elements	Electrical Size $\lambda_0 \times \lambda_0 = \lambda_0^2$	Isolation (dB)	ECC	Diversity gain dB
9	40 × 48	5.6–6.1 8.7–10.08	4	0.746 × 0.896 = 0.6684	> 25	< 0.05	> 9.99
10	52 × 52	4.2–13.2	4	0.728 × 0.728 = 0.5299	> 25	< 0.05	> 9.99
11	90 × 90	2.77–12	4	0.831 × 0.831 = 0.6905	> 15	< 0.1	> 9.97
13	58 × 58	3–16	4	0.58 × 0.58 = 0.3364	> 18	< 0.07	-
14	38 × 38	3.0–20	4	0.38 × 0.38 = 0.1444	> 17	< 0.08	-
15	40 × 40	3.1–11	4	0.4 × 0.4 = 0.16	> 20	0.002	-
16	34 × 34	2.5–11.6	4	0.283 × 0.283 = 0.08008	> 18	< 0.05	-
19	150 × 80	3.3 to 5.82	8	1.65 × 0.88 = 1.452	20	< 0.04	9.99
This work	34 × 25	3.3–6.3	4	0.374 × 0.275 = 0.1017	> 20	< 0.02	> 9.97

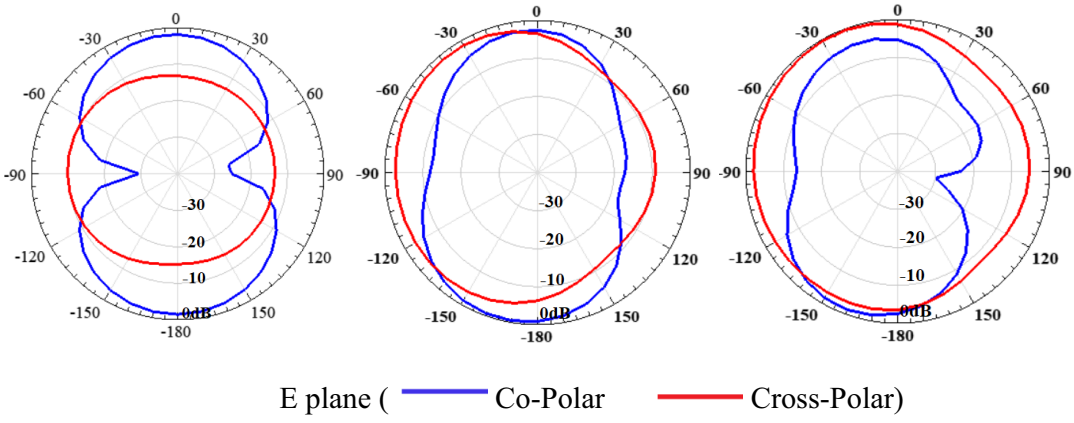

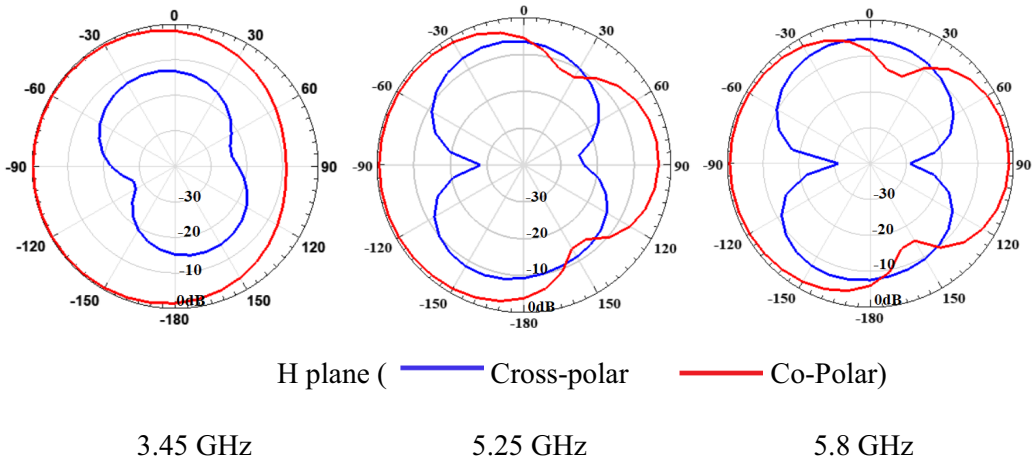

Figure 12. Radiation patterns of the proposed 4-elements MIMO antenna.

6. CONCLUSION

A compact four elements wideband MIMO antenna with high isolation using partial and separated ground for 5G sub-6 GHz applications is proposed. The novel structure employs neither any isolation techniques nor any meta-material or split ring resonator (SRR). It is simple to design and has small dimensions. To achieve high isolation, the structure is designed such that the surface current and near fields of left and right elements are concentrated toward left and right, respectively, whereas top and bottom elements are placed such that the interaction of near fields is minimum. The structure provides $S_{11} <= -10$ dB and mutual coupling < -20 dB over 3.3 to 6.3 GHz. ECC, TARC, DG, and MEG conform to MIMO standards. The antenna offers stable omnidirectional radiation patterns, thus suitable for 5G applications.

REFERENCES

1. Pirooj, A., M. N. Moghadasi, F. B. Zarrabi, and A. Sharifi, "A dual band slot antenna for wireless applications with circular polarization," *Progress In Electromagnetics Research C*, Vol. 71, 69–77, 2017.
2. Pirooj, A., M. N. Moghadasi, and F. B. Zarrabi, "Design of compact slot antenna based on split ring resonator for 2.45/5 GHz WLAN applications with circular polarization," *Microwave and Optical Technology Letter*, Vol. 58, 12–16, 2015.
3. Zarrabi, F. B., Z. Mansouri, N. P. Gandji, and H. Kuhestani, "Triple notch UWB monopole antenna with fractal Koch and T-shape stub," *AEU — Internationa.l Journal of Electronics and Communications*, Vol. 70, 64–69, 2015.
4. Heydari S., K. Pedram, Z. Ahmed, and F. B. Zarrabi, "Dual band monopole antenna based on metamaterial structure with narrowband and UWB resonances with reconfigurable quality," *AEU — International Journal of Electronics and Communications*, Vol. 81, 92–98, 2017.
5. Ullah, H., S. U. Rahman, Q. Cao, I. Khan, and H. Ullah, "Design of SWB MIMO antenna with extremely wideband isolation," *Electronics*, Vol. 9, 194, 2020.
6. Dkiouak, A., A. Zakriti, M. El Ouahabi, A. Zugari, and M. Khalladi, "Design of a compact MIMO antenna for wireless applications," *Progress In Electromagnetics Research M*, Vol. 72, 115–124, 2018.
7. Alsaif, H., "Extreme wide band MIMO antenna system for fifth generation wireless system," *Engineering, Technology & Applied Science Research*, Vol. 10, No. 2, 5492–5495, 2020.
8. Chaudhari, A. and R. K. Gupta, "A simple tri-band MIMO antenna using a single ground stub," *Progress In Electromagnetics Research C*, Vol. 86, 191–201, 2018.

9. Yalavarthi, U. D., R. T. Koosam, M. N. S. D. Venna, and B. Thota, "Four element square patch MIMO antenna for DSRC, WLAN, and X-band applications," *Progress In Electromagnetics Research M*, Vol. 100, 175–186, 2021.
10. Sereddy, C. R. and U. D. Yalavarthi, "Quad element tree shaped MIMO antenna for ultra-wide band applications," *Progress In Electromagnetics Research M*, Vol. 110, 197–209, 2022.
11. Alharbi, A. G., U. Rafique, S. Ullah, S. Khan, S. M. Abbas, E. M. Ali, M. Alibakhshikenari, and M.Dalarsson, "Novel MIMO antenna system for ultra wideband applications," *Applied Sciences*, Vol. 12, 3684, 2022.
12. Rayirathil, K., A. Mohan, and K. G. Padmasine, "A slotted compact four-port truncated ground structured MIMO antenna for sub-6 3.4 GHz 5G application," *Progress In Electromagnetics Research C*, Vol. 122, 267–277, 2022.
13. Kumar, P., S. Urooj, and F. Alrowais, "Design and implementation of quad-port MIMO antenna with dual-band elimination characteristics for ultra-wideband applications," *Applied Science*, Vol. 10, 1715, 2020.
14. Yin, W., S. Chen, J. Chang, L. Chunhua, and S. K. Khamas, "CPW fed compact UWB 4-element MIMO antenna with high isolation," *Sensors*, Vol. 21, 2688, 2021.
15. Ali, W. A. E. and A. A. Ibrahim, "A compact double-sided MIMO antenna with an improved isolation for UWB applications," *AEU — International Journal of Electronics and Communications*, Vol. 82, 7–13, 2017
16. Yang, Q., K. Wang, and Y. Sun, "Quad-port miniaturized ultra-wideband mimo antenna with metal vias," *Progress In Electromagnetics Research Letters*, Vol. 97, 95–103, 2021.
17. Zhou, H., D. W. M. Zhu, Y. Qiu, G. Yu, and H.-M. Zhou, "Wideband low-profile 8×8 MIMO antenna based IFA pair for ultrathin 5G smartphones," *Hindawi International Journal of Antennas and Propagation*, Vol. 2022, Article ID 5281470, 2022.
18. Hassan, W. M., K. M. Ibrahim, and A. M. Attiya, "MIMO antenna for N48, N77, N78 5G applications," *Progress In Electromagnetics Research C*, Vol. 117, 129–143, 2021.
19. Nithya, S. and V. Seethalakshmi, "MIMO antenna with isolation enrichment for 5G mobile information," *Hindawi Mobile Information Systems*, Vol. 2022, Article ID 1802352, 2022.
20. Piao, H., Y. Jin, and L. Qu, "A compact and straightforward self-decoupled MIMO antenna system for 5G applications," *IEEE Access*, Vol. 8, 129236–129245, 2020.
21. Patel, J., A. Desai, and T. Upadhaya, "Compact wideband four element optically transparent MIMO antenna for mm-wave 5G applications," *IEEE Access*, Vol. 8, 194206–194217, 2020.
22. Rosaline, I., A. Kumar, P. Upadhyay, and A. H. Murshed, "Four element MIMO antenna systems with decoupling lines for high-speed 5G wireless data communication," *Hindawi International Journal of Antennas and Propagation*, Vol. 2022, Article ID 9078929, 2022.
23. Rafique, U., S. Agarwal, N. Nauman, H. Khalil, and K. Ullah, "Inset-fed planar antenna array for dual-band 5G MIMO applications," *Progress In Electromagnetics Research C*, Vol. 112, 83–98, 2021.
24. Kumar, G. and K. P. Ray, *Broadband Microstrip Antennas*, Artech House, Norwood MA, 2003.
25. Ray, K. P., "Design aspects of printed monopole antennas for ultra-wide band applications," *International Journal of Antennas and Propagation*, Vol. 2008, 1–8, Article ID 713858, 2008.
26. Verulkar, S., A. Khade, M. Trimukhe, and R. K. Gupta, "Dual band split ring monopole antenna structures for 5G and WLAN applications," *Progress In Electromagnetics Research C*, Vol. 122, 17–30, 2022.
27. Sharawi, "Printed multi-band mimo antenna systems and their performance metrics [wireless corner]," *IEEE Antenna and Propagation Magazine*, Vol. 55, No. 5, 218–232, 2013.